Int. J. Microgravity Sci. Appl., **36** (3) (2019) 360301
DOI: 10.15011//jasma.36.360301

IIII Review IIII

Recent Accomplishment of "Group Combustion" Experiments aboard Kibo on ISS

Masato MIKAMI [1], Yasuko YOSHIDA[1], Takehiko SEO[1], Osamu MORIUE[2],
Tetsuya SAKASHITA[3], Masao KIKUCHI [3] and Yuji KAN[3]

Abstract

The first microgravity combustion experiments were conducted in 2017 aboard the Japanese Experiment Module "Kibo" on ISS, titled "Elucidation of Flame Spread and Group Combustion Excitation Mechanism of Randomly Distributed Droplet Clouds (Group Combustion)." The objective of this experiment is to study the effects of droplet interaction, radiative heat loss from a flame, and droplet motion during flame spread. This report describes some recent accomplishments from the "Group Combustion" experiments with droplet-cloud elements to study the effects of droplet interaction and randomly distributed droplet clouds with about 100 droplets to study the macroscopic characteristics of flame spread and local flame spread characteristics. Two types of anomalous behavior observed near the group-combustion-excitation limit are also reported, which had not been expected from parabolic flight experiments and percolation calculations to express the group-combustion excitation through flame spread over droplets.

Keyword(s): Space-based combustion experiment, Droplet cloud, Flame spread, Group combustion, Kibo/ISS.

Received 9 May 2019, accepted 14 June 2019, published 31 July 2019.

1. Introduction

The stable combustion of liquid fuels such as in aero engines requires the flame to spread to the fuel spray near the flame base and group-combustion excitation in the downstream region. The photograph in **Fig. 1** shows typical spray combustion. A number of droplets burns with a group flame surrounding them. This type of combustion is called group combustion. However, the flame-spread and group-combustion-excitation mechanisms have not yet been completely clarified.

The group combustion theory proposed by Chiu and co-workers[1)] is based on steady-state analysis and therefore cannot describe unsteady processes leading to group-combustion excitation. Mikami et al.[2)] observed the leading-flame region of a burning premixed *n*-decane spray/air in a counter flow. They found that group combustion is excited through the unsteady process of the flame spread to unburned droplets, leading to flame stabilization in a counter flow. Therefore, it is important to understand the group-combustion excitation mechanism through the flame spread over fuel droplets. In order to control the flame spread in the spray without relying on trial-and-error, we need to understand the flame spread mechanism and develop models and simulation methods that describe group-combustion excitation through flame spread

Our research group developed an original technique to generate droplets at intersections of 14-μm SiC fibers by supplying liquid fuel through fine glass needles[3)] and conducted flame-spread experiments on droplet arrays in microgravity to study the effects of ambient temperature[4)], ambient pressure[5-7)] and local droplet interaction[8, 9)], etc. **Figure 2** shows typical flame-spread behavior over a droplet array in microgravity. Furthermore, our research group proposed a new percolation model that employs flame spread between droplets as the local connection rule and describes flame spread over a randomly distributed droplet cloud as a complex system and studied the

Fig. 1 Spray combustion.

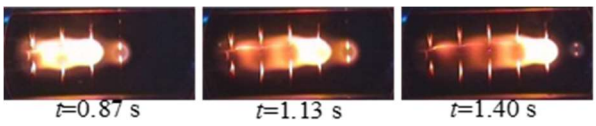

Fig. 2 Flame-spread behavior of linear *n*-decane droplet array in microgravity[3)].

1 Department of Mechanical Engineering, Yamaguchi University, 2-16-1 Tokiwadai, Ube, Yamaguchi 755-8611, Japan.
2 Faculty of Engineering, Kyushu University, 744 Motooka, Nishi-ku, Fukuoka 819-0395, Japan.
3 JEM Utilization Center, Japan Aerospace Exploration Agency, 2-1-1 Sengen, Tsukuba, Ibaraki 305-8605, Japan.
(E-mail: mmikami@yamaguchi-u.ac.jp)

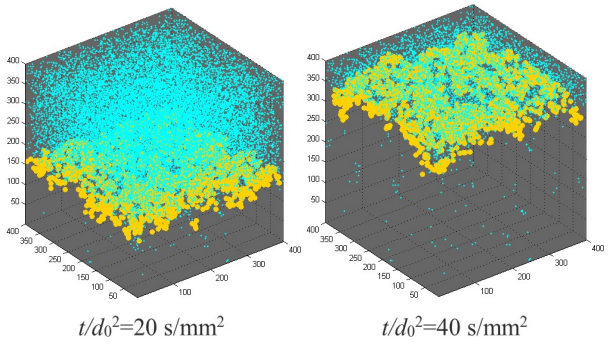

Fig. 3 Percolation calculation of flame-spread behavior for a dense droplet cloud[10].

Fig. 4 Mission patch of "Group Combustion" experiment aboard Kibo/ISS (source: JAXA).

group-combustion-excitation mechanism[10]. **Figure 3** shows typical flame-spread behavior over a randomly distributed droplet cloud. Although Umemura and Takamori[11] developed a percolation model to describe group-combustion excitation, the percolation model by Mikami et al.[10] focuses on the group-combustion-excitation limit. By microgravity science, this method deeply studies the microscopic thermal information transmission rule in the minimum system component that controls phenomena in complex systems and then enables us to understand the macroscopic characteristics of complex systems through the percolation model on the basis of the information transmission rule.

Kumagai and Isoda[12] started droplet combustion experiments in microgravity in the 1950s as the fundamental study of spray combustion. Droplet combustion experiments called FLEX and FLEX-2 were conducted in the US Experiment Module aboard the International Space Station (ISS)[13] and showed that a liquid hydrocarbon droplet of a few mm in initial diameter first vaporized with a hot-flame and then radiative extinction of the hot-flame occurred but the droplet vaporization continued with a cool-flame[14, 15]. Although there have been many interesting findings from droplet combustion researches in microgravity, they have not always been utilized to elucidate the spray combustion mechanism, and therefore a large gap still exists between them. In order to link knowledge from droplet combustion to elucidation of the mechanism of flame spread over randomly distributed droplet clouds considering the flame spread between droplets and finally to the elucidation of spray combustion mechanisms, our research group conducted droplet-cloud combustion experiments titled "Elucidation of Flame Spread and Group Combustion Excitation Mechanism of Randomly Distributed Droplet Clouds (Group Combustion)" in 2017 as the first combustion experiments aboard the Japanese Experiment Module "Kibo" on ISS[16-20]. **Figure 4** shows the mission patch of "Group Combustion" Experiments. The outer blue circle and yellow circle respectively represent the blue flame and yellow luminous flame of a single droplet; droplet-cloud combustion conducted aboard Kibo/ISS is shown in the lower part, and spray combustion is shown in the upper left part.

Since the droplet spacing is not uniform in spray due to the random dispersity of droplets, the flame spread in the droplet scale will be affected by local droplet interaction. The flame spread from the group flame to a droplet cluster will be affected by radiative heat loss depending on the cluster scale. Furthermore, the flame spread is possibly affected by free droplets since the droplets in spray are movable in space. "Group Combustion" Experiments aboard the Kibo/ISS studied these three effects on flame spread using high-quality long-duration microgravity, which have not yet been considered in the percolation model of flame spread in droplet clouds. The long-duration microgravity enabled us to generate randomly distributed large-scale droplet clouds, droplet-cloud elements, droplet-cluster arrays and movable droplets with high accuracy, which cannot be realized in short-duration microgravity on Earth, and to observe their combustion. This paper describes some recent accomplishments of the flame-spread experiments with droplet-cloud elements[19] and randomly distributed droplet clouds[17,18,20] that were conducted as parts of the "Group Combustion" Experiments aboard Kibo/ISS.

2. Group Combustion Experiment Module (GCEM)

The Group Combustion Experiment Module (GCEM) was used in this experiment. **Figure 5** shows GCEM. The droplet-cloud generation system and the ignition system were installed inside the combustion chamber. The droplet generation and burning behavior were observed by a digital camera through a glass window. Details of GCEM are reported in Refs. 21, 17, 18.

A 30×30 SiC-fiber lattice with a 4-mm interval of 14-μm SiC fiber (Nippon Carbon, Hi-Nicalon) was used to tether the droplets. *n*-Decane was supplied from a stepping-motor-driven syringe to the tip of the glass-tube needle. The position of the tip of the glass-tube needle was moved by a three-axis traverse system to

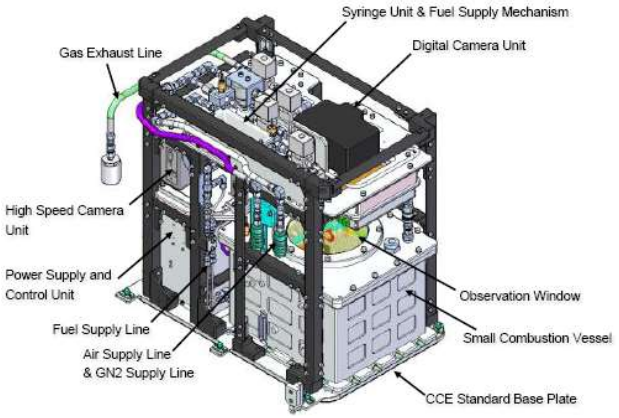

Fig. 5 Group Combustion Experiment Module (GCEM)[21].

generate the droplets at a predetermined lattice point. The droplets were generated one by one to form droplet-cloud elements and randomly distributed droplet clouds. In the case with randomly distributed droplet clouds, we made all the droplets have the same diameter at ignition by considering pre-vaporization of the droplets during the droplet-cloud generation. We obtained the vaporization-rate constant required to estimate the droplet diameter decrease due to pre-vaporization in the initial check-out phase of the "Group Combustion" Experiments. The details are described later in Subsection 4.1.

The flame spread of the droplet cloud was initiated by the hot-wire ignition of a droplet on one side of the lattice. A digital camera (Canon, EOS 5D Mark II) took still images of droplet clouds with an LED back-light to measure the initial droplet diameters and movies of burning behavior. The temperature around burning droplets was measured by the Thin Filament Pyrometry (TFP) method based on visible light emission from the SiC fiber tethering droplets[9]. As discussed in Refs. 3 and 23, the effect of the 14-μm SiC fiber on the flame spread is negligible.

GCEM was installed in the Chamber of Combustion Experiment (CCE) placed on the cold plate of the work volume of the Multi-purpose Small Payload Rack in Kibo. Thus the temperature near the droplet cloud was maintained at 293 K except during burning.

3. Effects of Droplet Interaction on Flame-Spread Limit[19]

Since the droplet spacing is not uniform in randomly distributed droplet clouds, the flame spread will be affected by local droplet interaction. As part of the "Group Combustion" Experiments, our research group conducted experiments on flame spread over the droplet-cloud element with uneven droplet spacing, which represents a local droplet pattern appearing in a

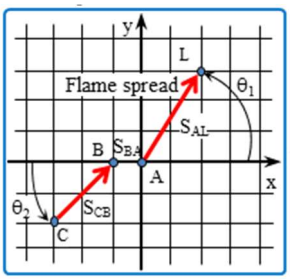

Fig. 6 Droplet-cloud-element model for flame spread from Droplet C to Droplet L via Droplets B and A[19].

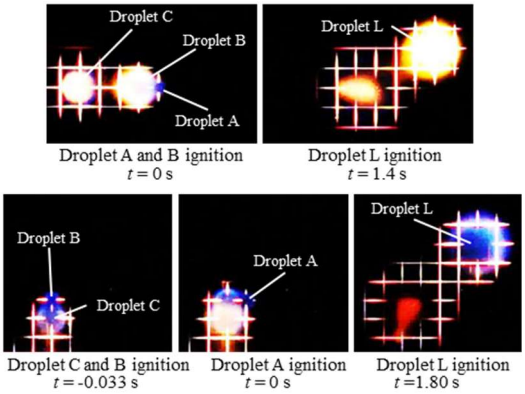

Fig. 7 Typical sequential photographs of the flame-spread behavior to Droplet L from the interactive burning of the two droplets Droplets B and A (top) and from the interactive burning of the three droplets Droplets C, B and A (bottom)[19].

randomly distributed droplet cloud near the group-combustion-excitation limit.

Figure 6 shows the droplet-cloud-element model. The droplet-cloud element consists of four droplets, Droplets C, B, A, and L. Droplet L is to check the flame-spread limit from burning Droplet A. Droplets B and C are employed to study the effect of droplet interaction with Droplet A. **Figure 7** displays typical sequential photographs of the flame-spread behavior to Droplet L from the interactive burning of the two droplets Droplets B and A and from the interactive burning of the three droplets, Droplets C, B and A. These types of flame-spread experiments were repeated with different positions of Droplet L to have the flame-spread-limit distributions. **Figure 8** shows the flame-spread-limit distributions around burning Droplet A with strong two-droplet interaction with Droplet B and with strong three-droplet interaction with Droplets C and B. The condition of the flame spreading to Droplet L is plotted as "○", the condition of no-flame spreading is plotted as "×". The flame-spread limit exists between ○ and ×. Both the horizontal axis and vertical axis are normalized by the average initial droplet diameter d_0. **Figure 8** shows the flame-spread-limit

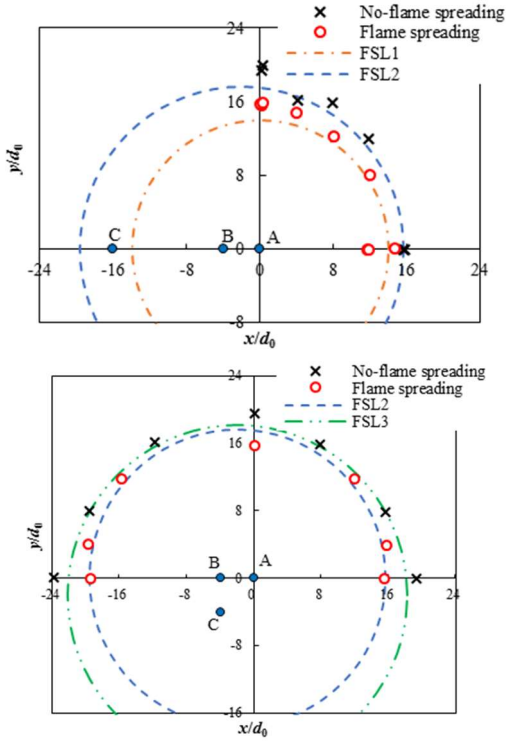

Fig. 8 Flame-spread-limit distributions for droplet spacings between Droplets C and B, S_{CB}/d_0=12 and between Droplets B and A, S_{BA}/d_0=4 (top) and for S_{CB}/d_0=4 and S_{BA}/d_0=4 (bottom)[19].

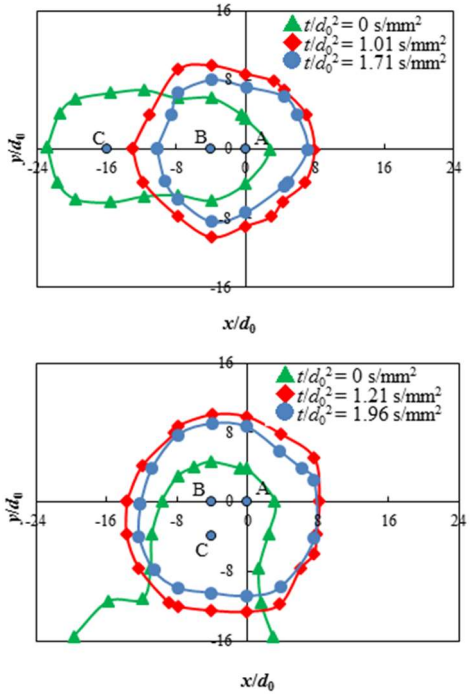

Fig. 9 Isothermal lines of 1200 K during the flame spread in the case without flame spreading to Droplet L[19].

distance around a single droplet, which is termed FSL1 and is $(S/d_0)_{limit}$=14[3], that around an imaginary droplet with twice the volume located at the center of the mass of Droplets B and A, which is termed FSL2 and is $2^{1/3}(S/d_0)_{limit}$, and that around an imaginary droplet with three times the volume located at the center of the mass of Droplets C, B and A, which is termed FSL3 and is $3^{1/3}(S/d_0)_{limit}$. **Figure 8** suggests that a flame-spread limit with strong two-droplet interaction exists outside FSL1, and almost coincides with FSL2 but is slightly inside FSL2. A flame-spread limit with strong three-droplet interaction exists between FSL2 and FSL3.

Figure 9 shows the isothermal line of 1200 K measured by the TFP method during the flame spread in the case that the flame does not spread to Droplet L. The time is expressed as the elapsed time from ignition of Droplet A normalized by the squared initial droplet diameter, t/d_0^2. Under both conditions, after a certain time from ignition of Droplet A, the high-temperature region becomes a circular shape centered at the center of the mass of the interactive droplets, i.e., Droplets B and A in the top figure of **Fig. 9** and Droplets C, B and A in the bottom figure of **Fig. 9**. This behavior coincides with the discussion considering FS2 and FS3.

Mikami et al.[23] experimentally studied the flame spread between uneven diameter droplets, from Droplet A to Droplet L, in microgravity and show that the flame-spread limit depends greatly on the burning lifetime of Droplet A. Yoshida el al.[19] extend this way of thinking to the analysis of the flame-spread limit with droplet interaction. **Figure 10** shows the dependence of the flame-spread-limit distance $(S_{ML}/d_0)_{limit}$ from the center of the mass of the interactive droplets on the burning lifetime t_{bA}/d_0^2 without flame spreading to Droplet L. $(S_{ML}/d_0)_{limit}$ exists between the flame-spreading conditions and the no-flame spreading conditions. In addition to the case with the strong three-droplet interaction, data in the case with the strong two-droplet interaction with different positons of Droplet C, θ_2=0 and 90 deg.,

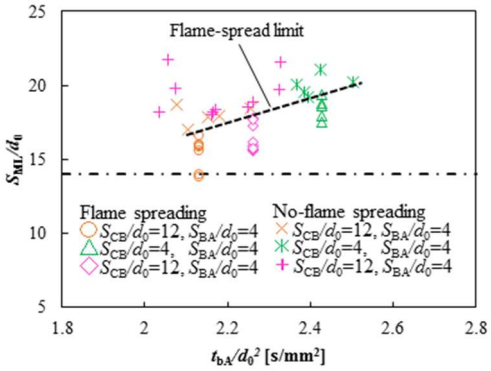

Fig. 10 Dependence of flame-spread-limit from the center of the mass of interactive burning droplets on the burning lifetime of Droplet A, t_{bA}/d_0^2 [19].

are also plotted. This figure suggests that the flame-spread limit from the imaginary droplet, Droplet M, located at the center of the mass of interactive droplets increases with an increase in the burning lifetime of Droplet A.

4. Flame Spread over Randomly Distributed Droplet Clouds

4.1 Generation of a Large-scale Droplet Cloud and Reproducibility of Droplet-cloud Generation and Flame Spread[17)]

Figure 11 shows a photograph of randomly distributed 97-*n*-decane droplets in GCEM aboard ISS. This photograph was taken at the hypothetical ignition time. It took longer than 20 minutes from the start of droplet generation of the first droplet untill the completion of droplet generation of the last droplet in the droplet cloud since the droplets were generated one by one as explained in Section 2. We made all the droplets have the same diameter at ignition by considering the pre-vaporization of the droplets during the droplet-cloud generation. Since no large-scale droplet-cloud generation has been conducted before in long-duration microgravity, the vaporization rate of a single droplet was measured first, then the droplet-cloud generation was conducted considering it, and the uniformity of the droplet diameter at ignition and its reproducibility were confirmed in the initial check-out phase of the "Group Combustion" Experiments aboard Kibo/ISS.

As fundamental vaporization data, we obtained the vaporization-rate constants for a single droplet and for the two interactive droplets at 293 K in microgravity by observing the droplet vaporization over 50 minutes. **Figure 12** shows *n*-decane droplets at 293 K in GCEM and d^2-t curves. The vaporization-rate constant was obtained from the slope of the least-square-fitted line for each condition. The vaporization-rate constants of the single droplet is K_S=0.000263 mm^2/s. The vaporization-rate constant of the two interactive droplets for droplet spacing at generation S/d_g=3.6 is K=0.000245 mm^2/s, which is somewhat smaller than K_S.

Next, a randomly distributed droplet cloud with 97 droplets was generated considering the vaporization-rate constant K_S of the single droplet, and the droplet diameters at the ignition timing, t=t_0, were examined. The diameter of the ith droplet, d_{gi}, at droplet generation timing, t=t_{gi}, was set as

$$d_{gi}^2 = d_0^2 + K(t_0 - t_{gi}) \qquad (1)$$

for d_0=1mm considering the droplet diameter decrease during the waiting time for ignition, t_0-t_{gi}. At first, K_S was used as K in Eq. 1 for all droplets. Then, we obtained the vaporization-rate constant K by assuming that all droplets had the same vaporization-rate constant in the droplet cloud and the droplet-diameter deviation, α_i, of ith droplet at ignition from the target diameter, d_0. Since the

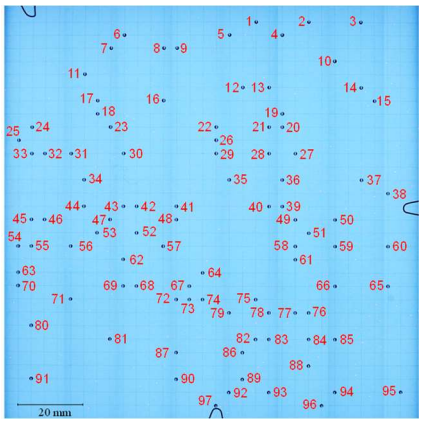

Fig. 11 Photograph of randomly distributed *n*-decane-droplet cloud generated by GCEM[17)]. The droplet number is also shown.

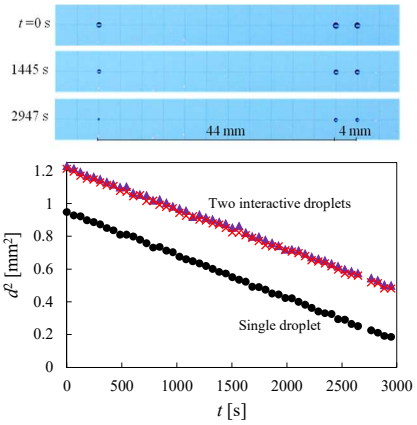

Fig. 12 Photograph of single and two interactive n-decane droplets. Temporal variations of droplet dimeter squared during vaporization of two *n*-decane droplets with S/d_g =3.6 and a single droplet at 293 K[17)].

droplets in the droplet cloud vaporize at smaller rates than that of a single droplet, K is smaller than K_S and therefore the droplet diameters at ignition deviate from the target diameter, d_0, if K_S is employed in Eq. 1.

Figure 13 plots α_i against the vaporization time, t_0-t_{gi}, for each droplet. α_i is expressed as

$$\alpha_i = (1-\gamma)K_S(t_0 - t_{gi})/(2d_0^2). \qquad (2)$$

where γ is the interaction coefficient of the droplet cloud, γ=K/K_S. The slope of the least-square fitted line of **Fig. 13** gives the interaction coefficient γ=0.65 and the vaporization-rate constant K=γK_S=0.00017 mm^2/s for the target diameter d_0=1 mm.

97-droplets with the same droplet arrangement as in **Fig. 11** were generated twice based on Eq. 1 with K==γK_S and γ=0.7 considering the uncertainty in obtaining γ from **Fig. 13**, and the

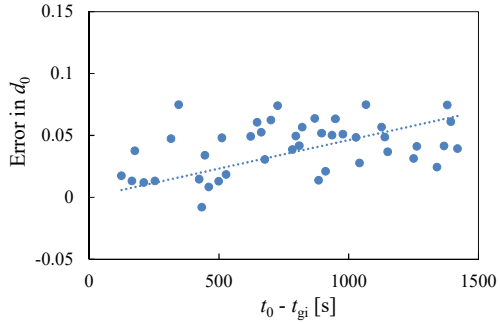

Fig. 13 Deviations of droplet diameter at ignition from the target diameter and waiting time for ignition after droplet generation[17].

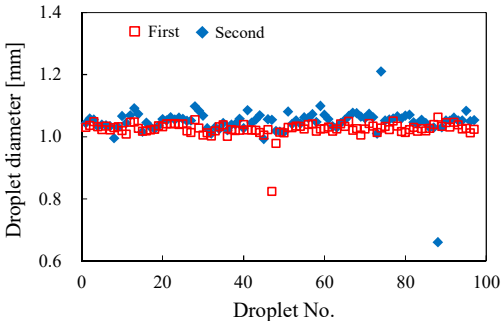

Fig. 14 Reproducibility of droplet diameter at ignition[17].

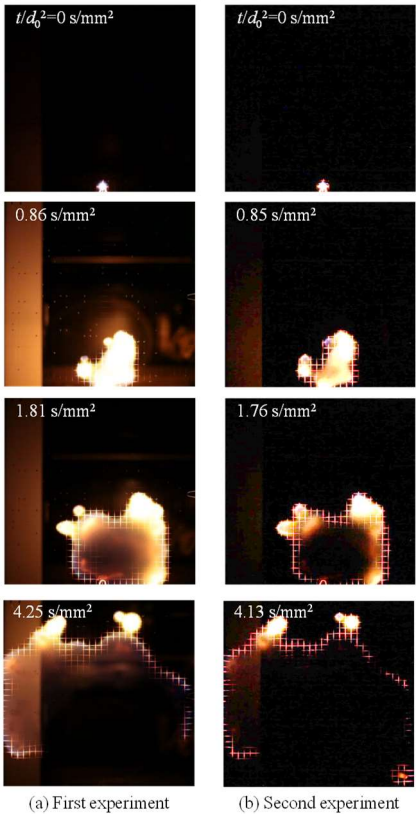

Fig. 15 Reproducibility of flame-spread behavior over a randomly-distributed droplet cloud[17].

flame-spread experiment was conducted twice. The droplet diameter at ignition d_0, i.e., the initial droplet diameter, is plotted against the droplet number for two experiments in **Fig. 14**. The mean droplet diameter and the relative standard deviation were respectively 1.03 mm and 2.4% in the first experiment and 1.05 mm and 4.5% in the second experiment. Although there were some droplets with a large deviation in d_0, the initial droplet diameter existed wholly within a certain range and therefore the reproducibility in the initial droplet diameter was satisfactory.

Figure 15 displays sequential photographs of the flame spread over the 97-droplet clouds for the two experiments. The elapsed time t from ignition is normalized by d_0^2, which is the square of the mean initial droplet diameter of the droplet cloud. The flame spread started from a small spherical flame around a single fuel droplet at t/d_0^2=0 and then spread across the droplet cloud until finally, a large-scale group flame appeared. Since the time difference for the same-phase flame-spread behavior occurrence was equal to or less than 3%, the reproducibility in the flame-spread behavior is considered satisfactory.

Lastly, we discuss the effect of pre-vaporization on the flame spread. “Group Combustion” Experiments used *n*-decane as the fuel. The temperature near the droplet cloud was maintained at 293 K during the droplet generation process. The equivalence ratio in the gas phase at the *n*-decane droplet surface is ϕ^+=0.09 at 293 K, which is lower than the lower flammability limit and is the maximum local equivalence ratio. A premixed-flame cannot propagate in such a very lean mixture. If a diffusion flame exists in such a very lean mixture, part of the fuel vapor contributes to the reaction only through the diffusion process. Since ϕ^+=0.09 corresponds to the fuel mass fraction Y_F=0.0006, which is much smaller than the fuel mass fraction in the gas phase at the droplet surface Y_F^+=0.85 in the quasi-steady burning condition, the effect of pre-vaporization on droplet burning is negligible. Nomura et al.[24] conducted flame-spread experiments in fuel vapor/air mixtures in microgravity and reported that such a small equivalence ratio does not affect the flame spread significantly.

4.2 Overall Flame-Spread Characteristics[18]

The group-combustion-excitation limit of randomly distributed droplet clouds and flame-spread characteristics near the excitation limit were investigated.

First, the number of droplets, M, varied from 152 to 67 for d_0=1 mm, and then the mean initial droplet diameter of the droplet cloud, d_0, varied from 1.1 to 0.9 mm for the same droplet arrangement with M=67. According to Mikami et al.[10], the mean droplet spacing $(S/d_0)_m$ of a droplet cloud was obtained as,

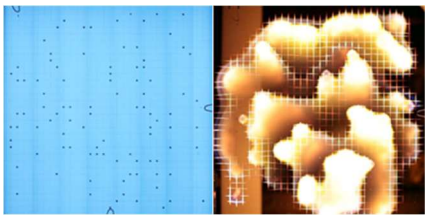

(a) $(S/d_0)_m$=11.9

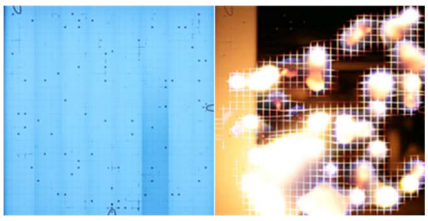

(b) $(S/d_0)_m$=14.5

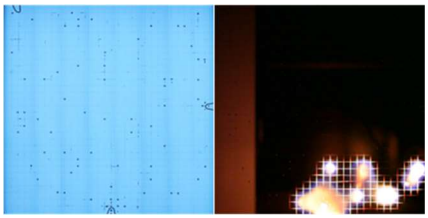

(c) $(S/d_0)_m$=16.2

Fig. 16 Backlit image of an initial droplet cloud and lighten-composite image of flame-spread behavior with 1-s intervals for different mean droplet spacings $(S/d_0)_m$ of randomly distributed droplet clouds[18].

$$(S/d_0)_m = (NL/d_0)/M^{1/2}. \quad (3)$$

where N is the number of lattice points on one side of the SiC-fiber lattice and L is the lattice-point interval of 4 mm.

Figure 16 displays backlit images of the initial droplet clouds and lighten-composite images of the flame-spread behavior with 1-s intervals for different mean droplet spacings $(S/d_0)_m$. In the case of $(S/d_0)_m$=11.9 shown in **Fig. 16a**, the flame spread starts from the ignition of the droplet close to the igniter in the central area of the lower side. An individual flame surrounding a single droplet merges with a group flame. The group flame grows into a large-scale group flame and finally reaches all sides of the lattice. The group flame spreads relatively radially but has a convex-concave irregular surface. In the case of $(S/d_0)_m$=14.5 shown in **Fig. 16b**, the flame-spread path becomes even more complicated. The flame does not spread to droplets in the upper left region. The group combustion, however, occurs based on the definition of group-combustion occurrence in the percolation model described by Mikami et al.[10] because the flame reaches all sides of the lattice. In the case of $(S/d_0)_m$=16.2 shown in **Fig. 16c**, however, the flame reaches only the right side of the lattice and partial burning occurs. This condition is outside the group-combustion-excitation limit. The group-combustion-excitation limit exists between the conditions shown in **Figs. 16b** and **16c**. Since

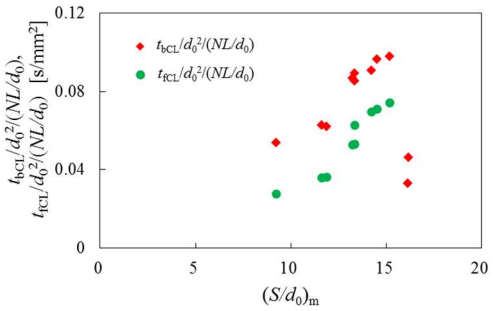

Fig. 17 Dependences of the burning lifetime of droplet cloud $t_{bCL}/d_0^2/(NL/d_0)$ and the flame-spread time required to reach a droplet on the upper side of the lattice $t_{fCL}/d_0^2/(NL/d_0)$ on the mean droplet spacing $(S/d_0)_m$ of a droplet cloud[18].

$(S/d_0)_m$=11.9 in **Fig. 16a** is close to the mean droplet spacing at the group-combustion-excitation limit obtained from a percolation calculation for droplet clouds distributed on a two-dimensional square lattice without considering the droplet interactive effect[10], the actual group-combustion-excitation limit exists at greater $(S/d_0)_m$.

Figure 17 shows the dependences of two characteristic times of burning droplet clouds on the mean droplet spacing $(S/d_0)_m$. The flame-spread time of the droplet cloud t_{fCL} is the time after ignition required for the flame to reach a droplet on the top side of the lattice. The burning lifetime of the droplet cloud t_{bCL} is the total burning time of the droplet cloud. Both times are normalized by d_0^2 and the lattice size NL/d_0. There is a maximum mean droplet spacing over which the flame cannot reach the top of the lattice and the group-combustion-excitation limit exists around it. The burning lifetime of the droplet cloud increases with $(S/d_0)_m$ first, attains maximum around the group-combustion-excitation limit and then rapidly decreases with an increase in $(S/d_0)_m$. According to the percolation theory[25], the characteristic time scale diverges at the critical point. The trend in the burning lifetime is conceivably similar to that. The number density of unburned droplets also attains maximum around the group-combustion-excitation limit.

According to a percolation calculation[26], the mean droplet spacing $(S/d_0)_{mcr}$ at the group-combustion-excitation limit for droplet clouds distributed on a two-dimensional square lattice is 11.4 without considering the droplet interactive effect and 13.5 considering the preliminary results of the flame-spread-limit extension with the two-droplet interaction[9]. However, **Fig. 17** shows that the mean droplet spacing, $(S/d_0)_{mcr}$, at the group-combustion-excitation limit is between 15.2 and 16.1, which is greater than the prediction.

Furthermore, we have analyzed the relationship between the flame-spread limit with droplet interaction and the local flame-spread limit in the flame spread of randomly distributed droplet clouds near the group-combustion-excitation limit[27].

4.3 Anomalous Behavior[18, 20)]

During the flame spread near the group-combustion-excitation limit, two types of anomalous behavior appeared: large-scale ignition and re-burning by a slow flame propagation in a burned area, which had not been expected from parabolic flight experiments[22)] and percolation calculations[10)].

Figure 18 shows flame-spread behavior with a large-scale ignition for the mean droplet spacing $(S/d_0)_m$=14.5, where the droplet pattern is the same as that shown in **Fig. 16b**. The same phenomenon occurred in the case for $(S/d_0)_m$=15.2, where the droplet pattern is the same but the averaged initial droplet diameter d_0 is different from the case shown in **Fig. 16b**. Near the group-combustion-excitation limit, the flame spreads along complicated paths. Therefore, the droplet cluster showing the large-scale ignition exists initially outside the flame-spread limit but vaporizes by heating from a group flame to form a flammable mixture. The ignition of the flammable mixture by a flame coming from another route probably causes the large-scale ignition.

Figure 19 shows the re-burning phenomenon by a slow-flame propagation in a burned area for $(S/d_0)_m$=13.3. The droplet pattern is the same as that shown in **Fig. 18**, but d_0=1.10 mm. The same phenomenon occurred in the case for $(S/d_0)_m$=12.1. As shown in **Fig. 19**, from t=6.93 s until t=7.27 s, a slow flame propagation occurs in the central area. The flame propagation is very slow, i.e., one tenth that of normal premixed flames, such as in the blue-flame propagation in the large-scale ignition observed at t=4.87-4.90 s in **Fig. 18**. It is not shown in **Fig. 19**, but the group flame has already passed the central area before the slow flame propagation occurs. In order for the flame to propagate in the burned area, there needs to be a flammable mixture. The slower propagation speed requires the burning of a leaner mixture or a diluted mixture. This anomalous behavior may be because a part of the group flame extinguished due to the excessive radiative heat loss, and then the unburned mixture diluted by the combustion products was ignited by a flame from another route.

Experiments with droplet-cloud elements were also conducted as parts of "Group Combustion" Experiments to test the hypotheses for two types of anomalous behavior[20)].

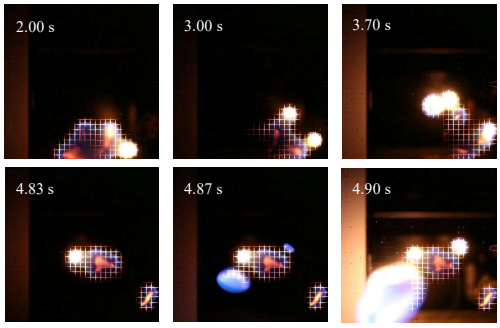

Fig. 18 Flame-spread behavior with a large-scale ignition for mean droplet spacing $(S/d_0)_m$=14.5[18)].

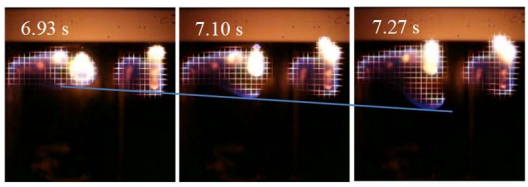

Fig. 19 Flame-spread behavior with a slow flame propagation in a burned area for mean droplet spacing $(S/d_0)_m$=13.3[20)].

5. Concluding Remarks

We investigated the effects of local droplet interaction on flame spread using two types of droplet systems arranged on a SiC-fiber lattice: droplet-cloud elements with two or three interactive droplets and randomly distributed droplet clouds with 67-152 droplets. The main findings and achievements are as follows:

(1) We developed a droplet-cloud generation method to control the droplet diameter at ignition based on the verification results obtained aboard the Kibo/ISS. This method enabled us to realize flame-spread experiments in high-quality, long-duration microgravity with randomly distributed large-scale droplet clouds, droplet-cloud elements, droplet-cluster arrays, and movable droplet arrays and to obtain high-quality data.

(2) The flame-spread-limit distribution around the interactive burning of two or three droplets is nearly spherical with the center at the center of the mass of interacting droplets and depends on the burning lifetime of the interacting droplets.

(3) The overall combustion characteristics have been clarified around the group-combustion-excitation limit for the flame spread of randomly distributed droplet clouds. The characteristic time scale of combustion and the number density of unburned droplets attain maximum around the group-combustion-excitation limit.

(4) In addition to the local interactive effect, the extension of the local flame-spread limit due to the droplet pre-heating associated with the complicated flame-spread path conceivably contributes to the extension of the group-combustion-excitation limit.

(5) We newly observed two anomalous combustion phenomena near the group-combustion-excitation limit: a large-scale ignition of a droplet cluster and re-burning by a slow flame propagation in a burned area.

Acknowledgements

This research was conducted as part of the Kibo utilization experiments called "Group Combustion" by JAXA and was also subsidized by JSPS KAKENHI Grant-in-Aid for Scientific Research (B) (18H01625).

References

1) H.H. Chiu and T.M. Liu: Combust. Sci. Technol., **17** (1977) 127.
2) M. Mikami, Y. Mizuta, Y. Tsuchida and N. Kojima: Proc. Combust. Inst., **32** (2009) 2223.
3) M. Mikami, H. Oyagi, N. Kojima, Y. Wakashima, M. Kikuchi and S. Yoda: Combust. Flame, **141** (2005) 241.
4) M. Mikami, H. Oyagi, N. Kojima, Y. Wakashima, M. Kikuchi and S. Yoda: Combust. Flame, **146** (2006) 391.
5) M. Mikami, N. Sano, H. Saputro, H. Watari and T. Seo: Int. J. Microgravity Sci. Application, **31** (2014) 172 (in Japanese).
6) N. Sano, N. Motomatsu, H. Saputro, T. Seo and M. Mikami: Int. J. Microgravity Sci. Application, **33** (2016) 330108.
7) K. Iwai, Y. Yoshida, N. Motomatsu, T. Seo and M. Mikami: Trans. JSASS Aerospace Tech. Japan, **16** (2018) 494.
8) H. Oyagi, H. Shigeno, M. Mikami and N. Kojima: Combust. Flame, **156** (2009) 763.
9) M. Mikami, H. Watari, T. Hirose, T. Seo, H. Saputro, O. Moriue and M. Kikuchi: J. Thermal Sci. Technol., **12** (2017) JTST0028.
10) M. Mikami, H. Saputro, T. Seo and H. Oyagi: Microgravity Sci. Technol., **30** (2018) 419.
11) A. Umemura and S. Takamori: Combust. Flame, **141** (2005) 336.
12) S. Kumagai and H. Isoda: Symp. Int. Combust., **6** (1957) 726.
13) D.L. Dietrich, V. Nayagam, M.C. Hicks, P.V. Ferkul, F.L. Dryer, T. Farouk, B.D. Shaw, H.K. Suh, M.Y. Choi, Y.C. Liu, C.T. Avedisian and F.A. Williams: Microgravity Sci. Technol., **26** (2014) 65.
14) V. Nayagam, D.L. Dietrich, P.V. Ferkul, M.C. Hicks and F.A. Williams: Combust. Flame **159** (2012) 3583.
15) T.I. Farouk and F.L. Dryer: Combust. Flame, **161** (2014) 565.
16) M. Mikami, M. Kikuchi, Y. Kan, T. Seo, H. Nomura, Y. Suganuma, O. Moriue and D.L. Dietrich: Int. J. Microgravity Sci. Appl., **33** (2016) 330208.
17) M. Mikami, H. Nomura, Y. Suganuma, M. Kikuchi, T. Suzuki and M. Nokura: Int. J. Microgravity Sci. Appl., **35** (2018) 350202.
18) M. Mikami, Y. Yoshida, T. Seo, T. Sakashita, M. Kikuchi, T. Suzuki and M. Nokura: Microgravity Sci. Technol., **30** (2018) 535.
19) Y. Yoshida, K, Iwai, K. Nagata, T. Seo, M. Mikami, O. Moriue, T. Sakashita, M. Kikuchi, T. Suzuki and M. Nokura: Proc. Combust. Inst., **37** (2019) 3409.
20) M. Mikami, Y. Yoshida, M. Kikuchi and D.L. Dietrich: Proc. 12th Asia-Pacific Conference on Combustion, (2019) ASPACC2019-1504.
21) M. Kikuchi, Y. Kan, A. Tazaki, S. Yamamoto, M. Nokura, N. Hanafusa, Y. Hisashi, O. Moriue, H. Nomura and M. Mikami: Trans. JSASS Aerospace Tech. Japan, **12** (2014) No. ists29, Th_25-Th_30.
22) Y. Yoshida, N. Sano, T. Seo, M. Mikami, O. Moriue, Y. Kan and M. Kikuchi: Int. J. Microgravity Sci. Appl., **35** (2018) 350203.
23) M. Mikami, N. Motomatsu, K. Nagata, Y. Yoshida and T. Seo: Combust. Flame, **193** (2018) 76.
24) H. Nomura, H. Takahashi, Y. Suganuma and M. Kikuchi: Proc Combust. Inst., **34** (2013) 1593.
25) D. Stauffer and A. Aharony: Introduction to Percolation Theory (Revised 2nd Ed.), CRC Press, (1994).
26) H. Saputro, T. Seo and M. Mikami: Proc.17th Annual Conference of ILASS-Asia, ILASS-Asia2014-058, (2014).
27) Y. Yoshida, K. Nagata, R. Uneyama, T. Seo, M. Mikami and M. Kikuchi: Proc. 56h Sym. Japanese Combust., (2018) D332 (in Japanese).